Chapter 3

TESLA Superconducting Linear Collider

TESLA Collaboration

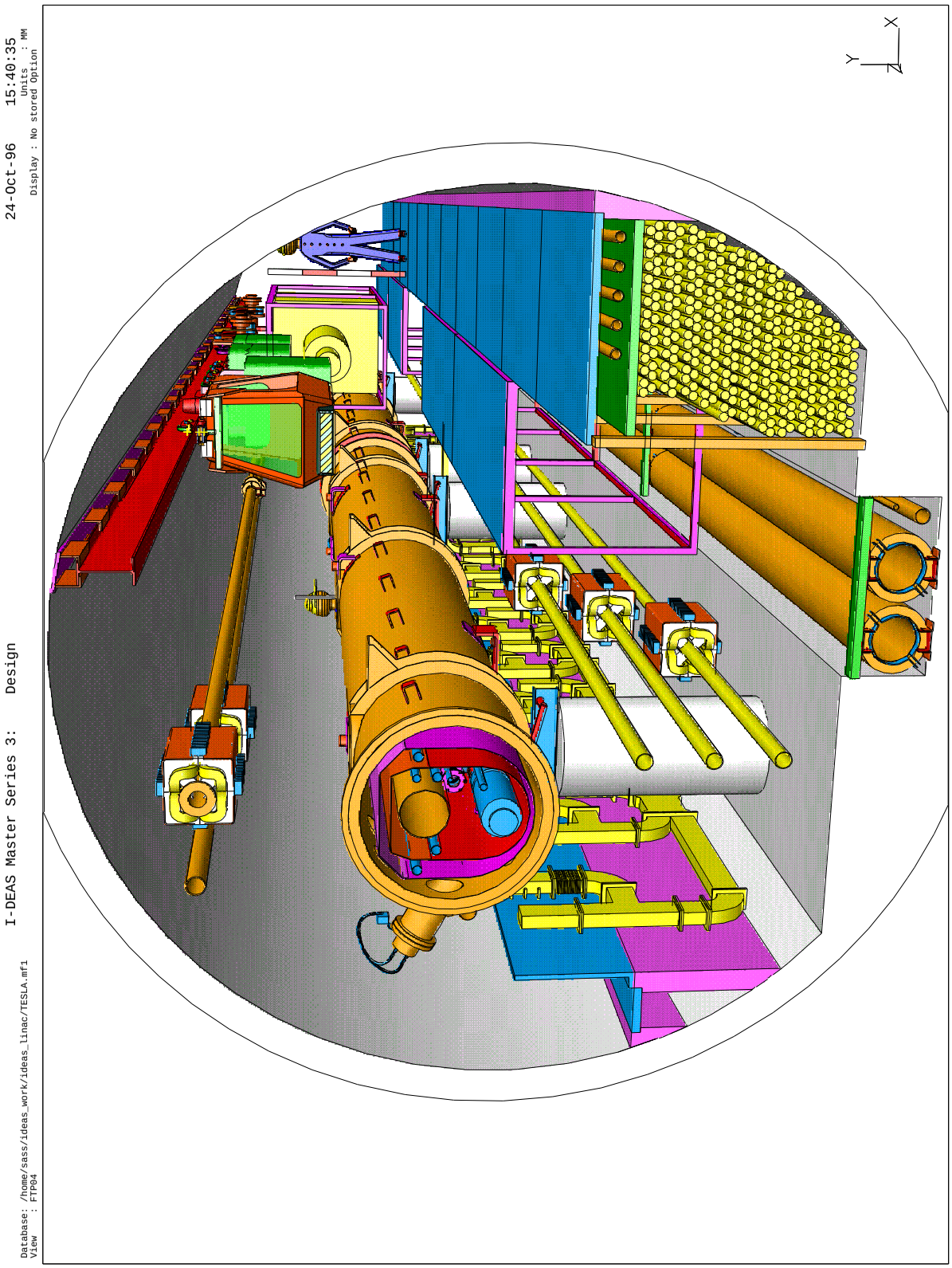
24-Oct-96 15:40:35
Units : MM
Display : No stored Option
I-DEAS Master Series 3: Design
Database: /home/sass/ideas_work/ideas_linac/TESLA.mf1
View : FTP04
Y
X
Z

Author List

DESY (coordinating Institute), Notkestr. 85, D-22603 Hamburg: I. Altmann, R. Bacher, R. Bandelmann, W. Bialowons, W. Bothe, R. Brinkmann (editor), H.-D. Brueck, H. Burmeister, M. Clausen, G. Csuka, G. Deppe, H. Dinter, A. Drozhdin (now at FNAL), B. Dwersteg, J. Eckoldt, D. Edwards, U. Engelke, K. Escherich, W. Eschricht, K. Flöttmann, P.D. Gall, A. Gamp, R. Glantz, A. Goessel, G. Grygiel, K. Hanke, O. Hensler, R. Hensler, G. Hoffmann, N. Holtkamp, G. Horlitz†, D. Hubert, J.P. Jensen, H. Kaiser, R. Kaiser, U. Knopf, R.-D. Kohaupt, G. Kreps, R. Lange, M. Leenen, H. Lierl, T. Limberg, F. Löffler, A. Matheisen, G. Meyer, W.-D. Möller, M. Pekeler, O. Peters, B. Petersen, P. Pillat, J. Pflüger, D. Proch, K. Rehlich, D. Renken, D. Reschke, H.-O. Roggenbuck, J. Roßbach, J. Rümmler, M. Sachwitz, T. Schilcher, M. Schmitz, P. Schmüser, B. Schoeneburg, H. J. Schreiber, S. Schreiber, D. Schulte (now at CERN), W. Schwarz, M. Seidel (now at SLAC), J. Sekutowicz, D. Sellmann, S. Simrock, W. Singer, K. Sinram, B. Sparr, M. Stolper, T. Stoye, K. Tesch, D. Trines, F.R. Ullrich, N. Walker, R. Wanzenberg, H.P. Wedekind, G. Weichert, H. Weise, J. G. Weisend, B. H. Wiik, S. G. Wipf, K. Wittenburg, J. Wojtkiewicz, S. Wolff, K. Zapfe-Düren;

Academy of Mining and Metallurgy, Krakow: K. Pieczora, Z. Sanok;

Beijing Institute of Vacuum Electronics: Lu Fuhai;

Budker INP, 670090 Novosibirsk: B. Grishanov;

Budker INP, Protvino Branch, 142284 Protvino, Moscow Region: V. Balakin, A. Sery;

CE Saclay, F-91191 Gif-sur-Yvette Cedex: B. Aune, S. Chel, J. Gastebois, M. Juillard, A. Mosnier, O. Napoly, A. Novokhatsky (on sabbatical leave from INP Novosibirsk), J.M. Rifflet;

CERN: D. Bloess, G. Cavallari, R. Fortin, E. Haebel;

Cornell University, Ithaca, NY 14853: H. Padamsee, M. Tigner;

FNAL, P.O. Box 500, Batavia, IL 60510: M. Champion, E. Colby, H. Edwards, D. Finley, M. Kuchnir, T. Nicol, T. Peterson, V. Shiltsev;

FZ Karlsruhe, D-76021 Karlsruhe: K.P. Jüngst, H. Salbert;

Helsinki University of Technology, Dep. of Mathematics, Otakaari 1, SF-02150 Espoo: E. Somersalo;

IHEP, 142284 Protvino, Moscow Region: P. Chevtsov, V. Gubarev, S. Goloborodko, O. Kourneev, M. Maslov, V. Sytchev, Y. Tchernoousko;

IHEP Beijing, PR China: Kong Xiang-Cheng, Yi Ding;

INFN Frascati, Via E. Fermi 40, I-00044 Frascati: M. Castellano, M. Ferrario, M. Minestrini, P. Patteri, F. Tazzioli;

INFN Milano, L.A.S.A., Via Fratelli Cervi 201, I-20090 Segrate: D. Barni, A. Bosotti, D.

Giove, P. Michelato, C. Pagani, P. Pierini, L. Serafini, G. Varisco;

INFN Sezione Roma2, Via della Ricerca Scientifica 1, I-00133 Roma: L. Catani, S. Tazzari;

INP Krakow: J. Baran, A. Bienkowski, M. Talach;

I.P.N. Orsay, F-91406 Orsay Cedex: S. Bühler, T. Junquera;

Institute of Modern Physics Lanzhou, PR China: , Ang Zheng-Ting;

LAL, F-91405 Orsay Cedex: R. Chehab, J. Gao, T. Garvey;

Max Born Inst., Postfach 1107, D-12474 Berlin: W. Sandner, I. Will;

Polish Academy of Science, Inst. of Physics, Al. Lotnikow 32/46, Pl-02-668 Warsaw: J. Krzywinski;

Rolf Nevanlinna Inst., University of Helsinki, P.O Box 4, SF-00014 Helsinki: J. Sarvas, P. Ylä-Oijala;

SEFT, Siltavuorenpenger 20c, SF-00170 Helsinki: R. Orava;

SLAC, P.O. Box 4349, Stanford, CA 94309: P. Emma;

Soltan Institute, Krakow: T. Plawski;

Tampere University of Technology, P.O. Box 692, SF-33101: A. Koski;

TH Darmstadt, Inst. f. Hochfrequenztechnik, Schloßgartenstr. 8, D-64289 Darmstadt: U. Becker, P. Schütt, M. Timm, T. Weiland;

Thomas Jefferson National Accelerator Facility, 12000 Jefferson Av., Newport News, VA 23606: P. Kneisel, C. Rode;

TU Berlin, Einsteinufer 17, D-10587 Berlin: H. Henke, R. Lorenz (now at DESY), I. Reyzl;

TU Dresden, Inst. f. Kälte u. Kryotechnik, D-01062 Dresden: M. Kauschke, H. Quack;

Johann-Wolfgang-Goethe Universität, Inst. f. Angewandte Physik, Robert-Mayer-Str. 2-4, D-60325 Frankfurt: H.-W. Glock, P. Hülsmann, H. Klein, W.F.O. Müller, C. Peschke;

Universität Wuppertal, FB Physik, Gauss-Str. 20, D-42119 Wuppertal: G. Müller, H. Piel;

University of California, Adv. Accelerator Physics Department, Los Angeles, CA 90024-1547: J. Rosenzweig;

Contents

3 TESLA Superconducting Linear Collider **275**

3.1 Overview . . . 281
3.1.1 Introduction . . . 281
3.1.2 General Layout . . . 286
3.1.3 Parameters at 500 GeV . . . 290
3.1.4 Upgrade to Higher Energy . . . 292
3.2 Linac Technology . . . 298
3.2.1 Cavity Design and Characteristics . . . 298
3.2.2 The Module . . . 320
3.2.3 Vacuum System . . . 333
3.2.4 RF Generation and Control . . . 336
3.2.5 Cryogenics . . . 365
3.2.6 Failure Handling . . . 377
3.3 Beam Dynamics . . . 387
3.3.1 Introduction . . . 387
3.3.2 Beam Optics . . . 387
3.3.3 Emittance Preservation . . . 389
3.3.4 Orbit Stability . . . 398
3.3.5 Summary Tolerances and Emittance Dilution . . . 400
3.4 Injection System . . . 403
3.4.1 Introduction . . . 403
3.4.2 Unpolarized Electron Source . . . 403
3.4.3 Polarized Electron Source . . . 404
3.4.4 Flat Beam RF Photocathode Electron Source . . . 408
3.4.5 Positron Source . . . 416
3.5 Damping Ring . . . 440
3.5.1 Introduction . . . 440
3.5.2 General Layout . . . 441
3.5.3 Beam Optics . . . 443
3.5.4 Rf-System and Collective Effects . . . 451
3.5.5 Injection and Extraction System . . . 454
3.5.6 Vacuum System . . . 455
3.6 Bunch Compressor . . . 460
3.6.1 Introduction . . . 460

3.6.2 Bunch Compressor Design Issues 460
3.6.3 Bunch Compressor Parameters 460
3.6.4 Bunch Compressor Optics 461
3.6.5 Peripheral Sections and the Full Beamline 462
3.6.6 Tolerances 465
3.7 Beam Delivery System 471
3.7.1 Introduction 471
3.7.2 Magnet Lattice and Optics 472
3.7.3 Sensitivity to Errors 478
3.7.4 Ground Motion 483
3.7.5 Phase Space Measurement and Tuning 489
3.7.6 Orbit and Spotsize Stabilisation 494
3.7.7 Beam-Beam Effects 496
3.7.8 Beam Collimation 498
3.7.9 Beam Extraction and Dump 506
3.8 Instrumentation and Controls 521
3.8.1 Beam Diagnostics 521
3.8.2 Beam Size Monitoring 532
3.8.3 Orbit Feedback 535
3.8.4 Control System 540
3.9 Survey and Alignment 551
3.9.1 Network on the Surface of the Earth 551
3.9.2 Requirements for the Aligment of the Components 551
3.9.3 Basic Alignment 551
3.9.4 Systematic Effects: Refraction of Air 552
3.9.5 Hydrostatic Levelling System 553
3.9.6 3–Point–Alignment–System 553
3.9.7 Transfering the Coordinates 555
3.10 Conventional Facilities and Site Considerations 556
3.10.1 Introduction 557
3.10.2 Overall Site Layout 557
3.10.3 DESY Site 560
3.10.4 Experimental Area 560
3.10.5 End Station 562
3.10.6 Cryogenic Halls 562
3.10.7 Tunnel Layout 562
3.10.8 Power Distribution 565
3.10.9 Water Cooling System 567
3.10.10 Air Conditioning and Ventilation 569
3.10.11 Fermilab as a Potential Site for the Linear Collider 570
3.11 Radiation Safety 586
3.11.1 Radiation Levels on the Earth Surface Above the Tunnel 586
3.11.2 Activation of the Main Beam Dump 587
3.11.3 Activations Outside the Tunnel 588

3.1 Overview

3.1.1 Introduction

As it has been discussed in chapter 1 of this report, studying electron-positron collisions at energies well beyond the reach of LEP ($E_{cm} \approx 200\,\mathrm{GeV}$) has a high potential for the future development of Particle Physics, in many respects complementary to the LHC. There is broad agreement in the High Energy Physics community that a linear e^+e^- collider with an initial center of mass energy of 350...500 GeV and a luminosity above $10^{33}\mathrm{cm}^{-2}\mathrm{s}^{-1}$ should be built as the next accelerator facility.

The feasibility of a linear collider has been demonstrated by the successful operation of the SLC, the only existing facility of this kind. Nevertheless, meeting the requirements for a next generation linear collider is by no means an easy task. In particular, high beam powers and very small spot sizes at the collision point are needed in order to obtain a sufficiently high luminosity. Several groups worldwide are pursuing different linear collider design efforts [1]. The fundamental difference of the TESLA approach compared to other designs is the choice of superconducting accelerating structures. The challenge of pushing the superconducting linac technology to a high accelerating gradient and at the same time reducing the cost per unit length, both necessary in order to be competitive with conventional approaches, is considerable, but the advantages connected with this technology (as summarized below) are significant and we are convinced that the potential for the machine performance is unrivaled by other concepts.

TESLA uses 9-cell Niobium cavities (Fig. 3.1.1) cooled by superfluid Helium to T=2K and operating at L-band frequency (1.3 GHz). The design gradient for a 500 GeV collider is g=25 MV/m with an unloaded quality factor of $Q_0 = 5{\cdot}10^9$. The design of the accelerating structures is described in detail in section 3.2.1.1. This technology provides several important advantages for the design of a linear collider. The power dissipation

	S-band	X-band	Two-beam	TESLA
Accelerating gradient [MV/m]	17	29...55	78	25
RF-frequency [GHz]	3	11.4	30	1.3
RF-peak power [MW/m]	12	50...100	144	0.2
Av. beam power [MW]	7.3	4	4	8.2
Beam pulse length [μs]	2	0.1	0.006	800
Bunch spacing [ns]	6	1.4	0.67	708
Vertical spot size at IP [nm]	15	5	7	19
Luminosity [$10^{33}\mathrm{cm}^{-2}\mathrm{s}^{-1}$]	5	6	5	6

Table 3.1.1: *Parameters for different 500 GeV linear collider designs. A more detailed discussion of the TESLA parameters is given in section 3.1.3.*

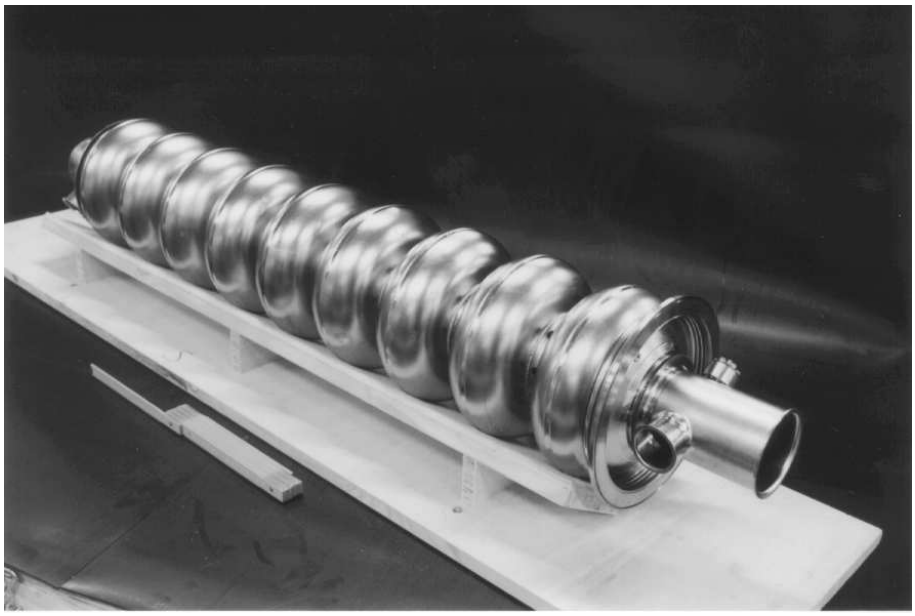

Figure 3.1.1: *The 9-cell Niobium cavity for TESLA.*

in the cavity walls is extremely small which allows to produce the accelerating field with long, low peak power RF-pulses and yields a high transfer efficiency of RF-power to the beam. With a high average beam power, the required luminosity can be achieved with a spot size at the interaction point (IP for short) only moderately (about a factor of 3.5) smaller than what has been achieved at the Final Focus Test Beam experiment performed at the SLAC linac [2]. At the same time the AC power consumption remains within acceptable limits (100 MW). The long RF-pulse allows for a large bunch spacing (see Table 3.1.1), making it easy for the experiment to resolve single bunch crossings. In addition, a fast bunch-to-bunch feedback can be used to stabilise the orbit within one beam pulse, which makes TESLA practically immune to mechanical vibrations which could otherwise lead to serious luminosity reduction via dilution of the spot size and separation of the beams at the IP. Further benefits of the long pulse are the possibility to use a head-on collision scheme with large-aperture superconducting quadrupoles in the interaction region and to employ a safety system which can "turn off" the beam within one pulse in case an emergency is indicated by enhanced loss rates.

The choice of a low drive frequency for TESLA results in very small transverse and longitudinal wakefields in the accelerating structures. This leads to relatively relaxed alignment tolerances for the linac components required for the transportation of a low emittance beam. Beam dynamics issues are discussed in detail in section 3.3, but it is instructive here to compare the different linear collider design concepts on a basis of simple scaling arguments [3]. One of the most essential contributions to emittance dilution results from short-range transverse wakefields due to random offsets of the accelerating structures with respect to the beam orbit. The emittance dilution from this effect can be written as

$$\frac{\Delta\epsilon}{\epsilon} \propto F \cdot \bar{\beta} \cdot \delta y_c^2 \tag{3.1.1}$$

where $\bar{\beta}$ denotes the average β-function in the linac (the stronger the focussing, the smaller $\bar{\beta}$), δy_c the rms-offset of the structures and F the dilution factor which depends on the beam parameters and very strongly on the linac frequency f_{RF}:

$$F \propto \frac{N_e^2 \sigma_z f_{RF}^6}{g^2 \epsilon_y} \tag{3.1.2}$$

The considerable variation of F for different linear collider designs is shown in Fig. 3.1.2. It becomes clear that TESLA can afford very much relaxed requirements for the alignment tolerances and for the beam optics. We consider it a crucial point to have a large safety margin concerning beam stability in order to be able to guarantee efficient and stable operation of such a future facility. In addition, part of the safety margin can be used to upgrade the machine performance beyond the "standard" requirements for the next generation linear collider. This point is discussed in more detail in sections 3.1.3 and 3.1.4.

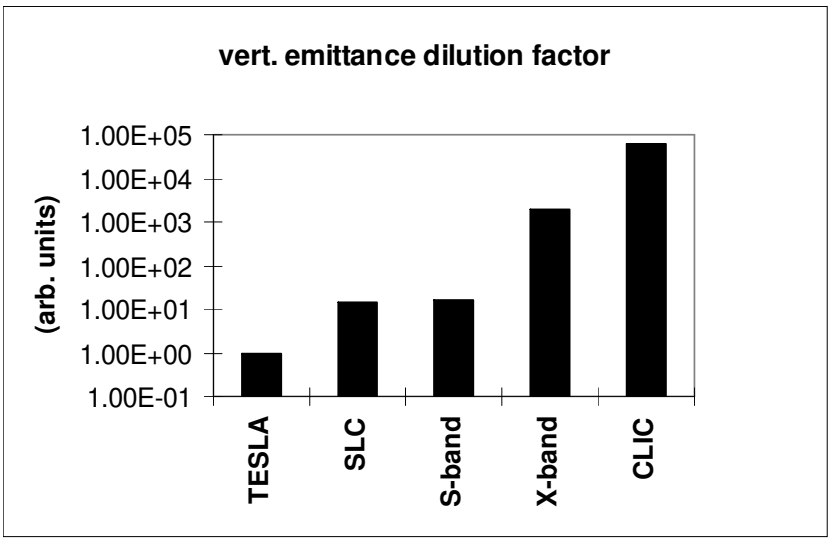

Figure 3.1.2: *Wakefield emittance dilution factor for different 500 GeV linear collider designs. The SLC is included for comparison.*

In order to demonstrate the feasibility of the s.c. cavity technology, the TESLA collaboration decided to start an R&D program and to build the TESLA Test Facility (TTF) several years ago [4]. In the formative stages of the TESLA collaboration, three 5-cell L-band cavities were built and tested to reach accelerating fields of 26-28 MV/m [5]. The TTF [6] includes the infrastructure for applying different processing techniques to the Niobium cavities obtained from industrial series production. At the time of writing this report, 12 cavities have been processed and tested at the TTF. Several of the cavities have reached or even surpassed the TESLA goal, see Fig. 3.1.3

for an example. A test linac is under construction incorporating 32 cavities in order to demonstrate acceleration of a beam up to 800 MeV. Operation with an RF- and beam-pulse structure as in the linear collider design is foreseen, so that a full integrated system test relevant for TESLA-500 is possible. While construction work on the TTF linac and commissioning of its first stage is in progress, several important results have already been obtained (see section 3.2.1.1 for more details on the status of cavity research):

- Several of the cavities have reached or even surpassed the TESLA goal, see Fig. 3.1.3 for an example.
- Field emission has been overcome by handling the cavities in a dust-free environment and by proper treatment.
- Gradients and quality factors achieved in horizontal tests were similar to those achieved in vertical tests.

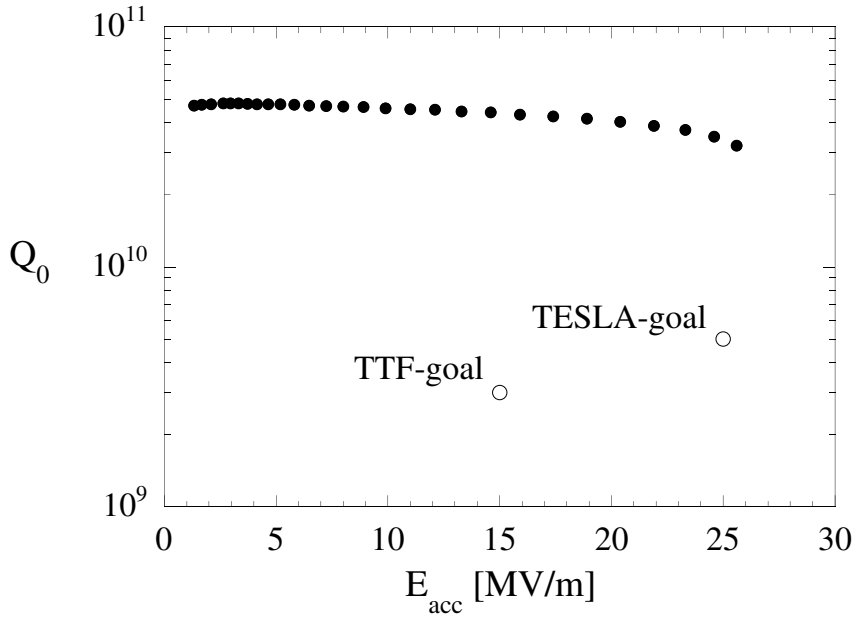

Figure 3.1.3: *Quality factor vs. accelerating gradient for one of the 9-cell TESLA cavities tested with CW-RF in a vertical cryostat. The initial goal for the TTF and the design goal for TESLA are indicated.*

While demonstration of a successfully working superconducting linac system is the primary goal at the TTF, its construction will also provide a sound basis for a cost analysis. Studies of cost effective component design are under way and the preparation of a detailed cost model for all major components and sub-systems of TESLA will be

the next step of our design work. There are, however, already important ingredients for a substantial cost reduction in the design of the systems.

One measure is to build cavities with a larger number of cells than done before (9 cells instead of typically 4-5 cells). Longer structures with higher number of cells lead to a reduced number of input couplers, HOM-couplers, tuning devices, RF-waveguides, etc. Building long cryostats with many cavities (there are 8 cavities per cryostat in the TTF design) also contributes to a reduction of the system costs. A large number of cryostats is grouped together in a 2.5 km long cryogenic unit for the TESLA linac. The helium distribution system is incorporated in the cryostats with only one feedbox every 2.5 km. The number of cold-to-warm transitions, which are costly because of the penetration of the heat shields and the vacuum vessel and which also contribute to the heat load, is reduced to a minimum.

X-Ray FEL and Further Options

Due to its ability to sustain highest beam quality during acceleration, the TESLA linac is the ideal driver for an X-ray Free Electron Laser (FEL). Such a device is now considered by the major part of the synchrotron radiation community as a truely new generation of X-ray sources. It is explained in chapter 5 of this report how an X-ray FEL can be integrated into TESLA, allowing to operate this facility in parallel with the linear collider.

The X-ray FEL concept represents a considerable extrapolation of present day FEL technology. It has therefore been decided to perform a proof-of-principle experiment at the TTF. After a successful test at about 50 nm wavelength, an energy upgrade of the TTF will open up the possibility to build a soft X-ray FEL user facility. Thus operational and scientific experience can be gained which seems indispensable for the construction of a large-scale X-ray FEL laboratory. Furthermore, a long-term adequate usage of the TTF will be provided.

If the linear collider is constructed close to an existing large proton storage ring (as the HERA-p ring or the TEVATRON), a linac-ring electron-proton collider with a center-of-mass energy of about 1 TeV is a possible option. There is also the possibility to convert the electron beam into a γ-beam by Compton scattering, thus obtaining γ-p collisions. The most serious issue here concerns the achievable luminosity (see e.g. refs. [8, 9, 10]). More detailed studies are required before a conclusion concerning the feasibility of a linac-ring e-p collider with reasonably high luminosity can be drawn.

Recently, the concept of $\mu^+\mu^-$ colliders has attracted much attention. While many design aspects of such a facility are still under study [11], it is already clear that a superconducting linac, operated in a multi-pass recycling mode, would be required. One may thus consider TESLA as the only linear collider which can be extended into a $\mu^+\mu^-$ collider in the long-term future, provided this approach towards multi-TeV lepton colliders is found to be feasible and superior to e^+e^- machines in this energy range.

In case TESLA is constructed at the DESY site, an additional option becomes attractive. The HERA electron ring can be used as a pulse stretcher to deliver a con-

tinuous electron beam of 15...25 GeV for Nuclear Physics experiments (see appendix B). The ring is filled by additional beam pulses generated in the lower energy part of one of the TESLA linacs. The additional investment required for this option would be minimal, still the quality of the beam delivered from the stretcher ring being comparable to the original ELFE proposal [7] for a continuous beam facility.

3.1.2 General Layout

A sketch of the overall layout of the TESLA linear collider is given in Fig. 3.1.4. We start the description of the various subsystems of the machine at the beam sources.

With the relatively large design beam emittance, it may be possible to obtain the required electron beam quality directly from a laser-driven RF gun. This design aspect is not fundamental but considered as a possible low-cost version of the electron injection system for an initial stage of operation. An additional damping ring, similar to the one on the positron side (see below), is likely to be required in order to exploit the full potential of the collider with smaller beam emittance. A polarized electron source with a larger emittance is used in that case (section 3.4.3). The requirements for longitudinal bunch compression are rather moderate and can be met with a single stage compressor, as described in section 3.6. After the bunch compressor, injection into the main linear accelerator takes place at a beam energy of 3.2 GeV.

The positron injection system has to provide a total charge of about $4 \cdot 10^{13} e^+$ per beam pulse, which does not seem feasible with a conventional source. The method considered here is to produce the positrons from γ-conversion in a thin target (section 3.4.5). The photons are produced by passing the spent high-energy electron beam after the IP through a wiggler. This requires a special beam-optical system and various collimators in order to deliver an electron beam of sufficiently small size to the wiggler. After the wiggler the electron beam is deflected, bypasses the photon target and is sent on a dump. The positrons are preaccelerated in a conventional 200 MeV L-band linac, followed by a 3 GeV superconducting accelerator. The method proposed here has a lower limit for the electron beam energy required to generate photons of sufficiently high energy. This limit is at about 150 GeV, which puts a lower boundary on the center-of-mass energy accessible with TESLA at maximum luminosity. In case lower energy running at high luminosity becomes important, solutions with additional electron beam pulses and bypass-beamlines are conceivable.

A low-intensity auxiliary e^+ source will be needed for commissioning and machine study purposes. We assume that the auxiliary source should be capable of generating single bunches at full design intensity and bunch trains at a few per cent of the design intensity.

Changes of the beam parameters at the IP can introduce fluctuations of the positron production efficiency, which in turn feed back to the spent beam properties via the collision at the next pulse. It has been checked that the coupled dynamical system is damped and stable and that the expected fluctuations are acceptable.

Besides providing a sufficiently high positron beam intensity, this concept offers additional advantages. With a thin target, the positron beam tends to have a smaller

transverse emittance than from a conventional source. The considerable investment and operating costs for a high-power electron linac needed in a conventional scheme are avoided. Furthermore, it is conceivable to obtain a polarized positron beam by using a helical undulator instead of a wiggler. This option is more ambitious concerning the required quality of the spent beam passing through the undulator.

The positron beam is injected into the damping ring at an energy of 3.2 GeV. The bunch train is stored in the ring in a compressed mode, with the bunch spacing reduced by about a factor of 14. Still a large ring circumference of about 17 km is required. We choose a damping ring design (section 3.5) here which avoids having to build an additional ring tunnel of this size. The layout has two 8 km straight sections, entirely placed in the main linac tunnel. Additional tunnels are only required for the small loops at the ends. Despite its unconventional shape (it has been named the "dogbone ring"), no particular difficulties concerning single particle and collective beam dynamics were found. A 400 m long wiggler section is foreseen to achieve sufficient damping. Special kicker devices are required for compression and decompression of the bunch train at injection and extraction, respectively. The two main linear accelerators comprise about ten thousand one meter long superconducting cavities each. Groups of 8 cavities are installed in a common cryostat, a cost-efficient modular solution which is already applied at the TTF linac (see section 3.2.2). Superconducting magnets for beam focussing and steering, beam position monitors and absorbers for higher order modes induced by the beam are integrated in the modules.

The RF-power is generated by some 300 klystrons per linac, each feeding 32 9-cell cavities. The required peak power per klystron is 8 MW, which includes a margin for correcting phase errors which occur during the beam pulse due to mechanical deformations of the cavities (Lorentz force detuning, microphonics). The high-voltage pulses for the klystrons are provided by conventional type modulators, or, as an alternative option presently under study, in "SMES" devices where the pulse energy is stored as magnetic field energy in superconducting solenoids. The TESLA RF-system is described in detail in section 3.2.4.

The cryogenic system of the TESLA linac is divided into 2.5 km long subsections, each supplied by a cryogenic plant, see section 3.2.5 for details.

The beam transport between the linac and the IP (so-called beam delivery system, described in section 3.7) consists of collimation, beam diagnostics and correction, and final focus sections. In the interaction region, no crossing angle is required, because the beams can be separated by an electrostatic deflector well before the first parasitic interaction with the subsequent bunch would occur (at 150 m from the IP). Large aperture superconducting quadrupoles can be used in the IR, with one benefit being that collimation requirements upstream for protection of the experiment from background are rather relaxed. With gas scattering practically absent in the TESLA linac and wakefields being very small, the expected amount of beam halo which must be collimated is small so that background from muons originating at the collimators is unlikely to be a problem. In case the loss rates at the collimators exceed an acceptable limit (e.g. due to mis-steering or possible failures upstream), the large bunch spacing allows to trigger a safety system which sends the remaining bunch train to a beamdump.

The concept of the final focus sytem is essentially the same as for the successfully tested FFTB system at SLAC. Beam size demagnification and chromatic corrections for the TESLA design parameters are even somewhat less ambitious than at the FFTB. The beams can be kept in collision at the IP with high accuracy by using a fast bunch-to-bunch feedback which measures the beam-beam deflection and steers the beams back into head-on collision within a time small compared to the beam pulse length. A similar system is foreseen at the entrance to the main linac and at its end, removing possible pulse-to-pulse orbit jitter generated in the injection system or in the linac.

The layout of the beam delivery system chosen here is optimized for a single interaction point. It can be entirely accomodated in a straight tunnel and is kept as simple as possible, with benefits for the required tunnel length (about 2.3 km for the total system between the two linacs) and for facilitating commissioning and operation of the machine. There is no fundamental problem arranging a 2nd IP by adding another beam line as sketched in Fig. 3.1.4. The detailed geometry and beam optics will depend on whether the 2nd experiment is to study e^+e^- collisions as well, or is aiming at the investigation of $\gamma\gamma$ and $e\gamma$ collisions. A discussion of the latter option for TESLA is given in appendix A. The two linear accelerators as well as the beam delivery system will be installed in an underground tunnel of 5 m diameter, see Fig. 3.1.5 and section 3.10. A $30 \times 80m^2$ experimental hall is foreseen to accomodate the detector, with an option to be extended in case a 2nd separate experiment is to be installed. Six additional surface halls are required at a distance of about 5 km along the linacs, each housing two cryogenic plants. These halls are connected to the underground tunnel by access shafts. They will also contain the modulators which generate the HV pulses for the klystrons. The pulse transformers are placed in the tunnel close to the klystrons and are connected to the modulators by cables. The long cables contribute to a few % of power losses, but it is advantageous that maintenance of the modulators will be possible while the machine is running without the need of access to the tunnel. Exchange of klystrons requires to interrupt operation of the machine. With an energy surplus of 2% foreseen in the design, such maintenance breaks of one day are necessary only every few weeks, assuming an average klystron life time of 40,000 h.

The layout of all subsystems of TESLA takes safety margins into account, as will become more clear by the detailed descriptions given in the respective sections of this report. Examples for safety margins are a 50% excess of the cooling capacity of the cryogenic plants and a 25% higher klystron peak power than what is needed according to the design parameters. In addition, margins concerning the beam parameters as emittances and bunch intensity are foreseen to allow for dilutions and losses at different stages from the source to the IP.

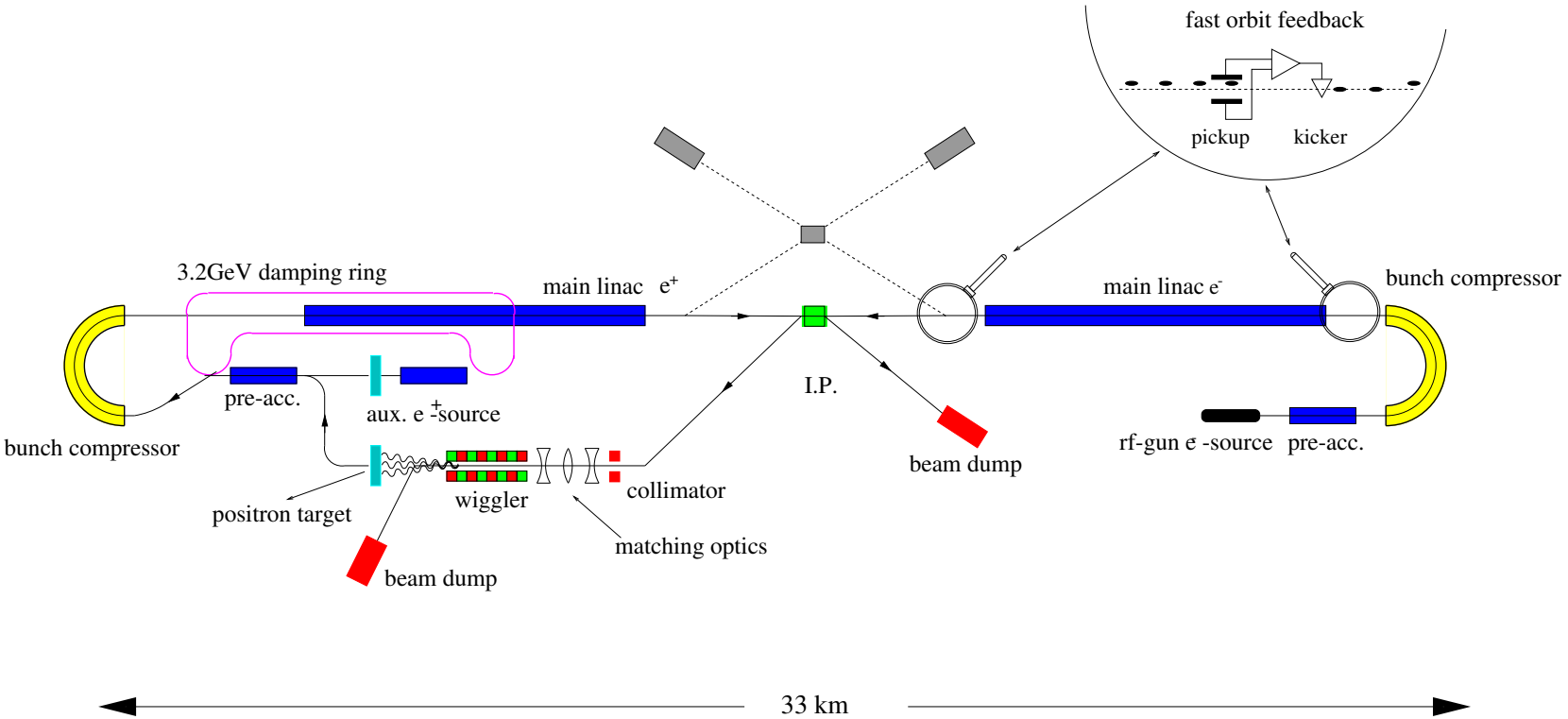

Figure 3.1.4: *Sketch of the overall layout of TESLA.*

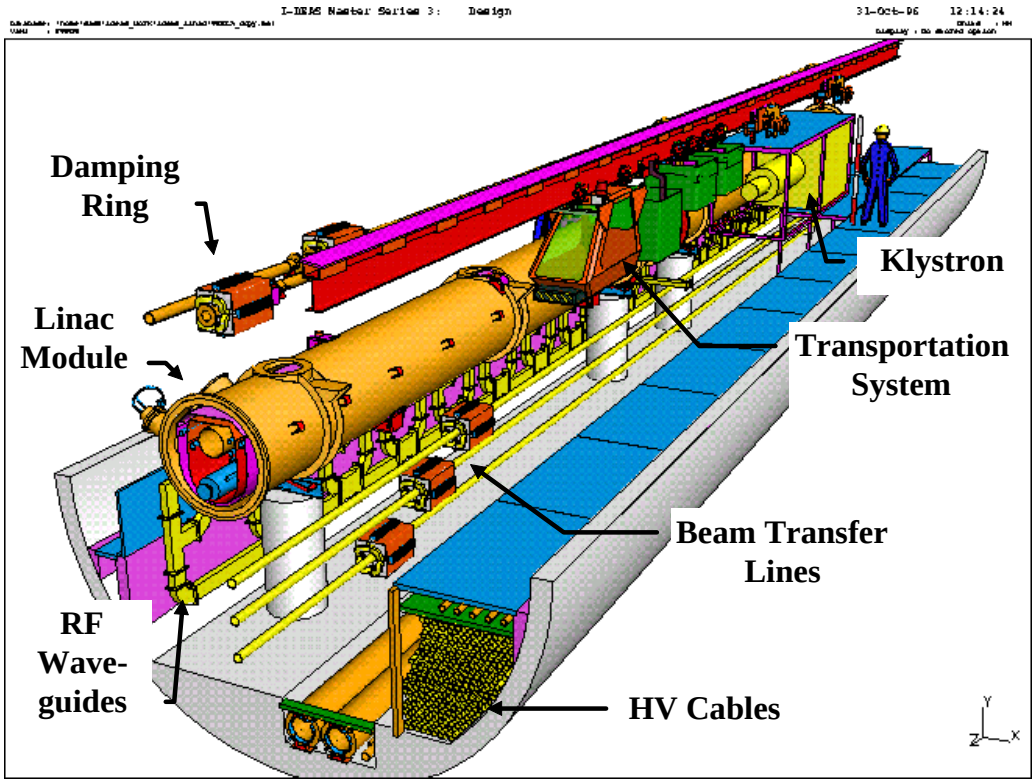

Figure 3.1.5: *Sketch of the 5 m diameter TESLA linac tunnel.*

3.1.3 Parameters at 500 GeV

The second key parameter for a linear collider, besides the center-of-mass energy of the colliding beams, is the luminosity L. It is given by

$$L = \frac{n_b N_e^2 f_{rep}}{4\pi\sigma_x^*\sigma_y^*} \times H_D \tag{3.1.3}$$

n_b	number of bunches per pulse
N_e	number of electrons (positrons) per bunch
f_{rep}	pulse repetition frequency
$\sigma^*_{x,y}$	horizontal (vertical) beam size at interaction point
H_D	disruption enhancement factor (typically $H_D \approx 1.5$)

Introducing the average beam power $P_b = E_{cm} n_b N_e f_{rep}$, the luminosity can be

written as

$$L = \frac{P_b}{E_{cm}} \times \frac{N_e}{4\pi\sigma_x^*\sigma_y^*} \times H_D \tag{3.1.4}$$

An important constraint on the choice of interaction parameters is due to the effect of beamstrahlung: the particles emit hard synchrotron radiation in the strong space-charge field of the opposing bunch. The average fractional beam energy loss from beamstrahlung is approximately given by [12]:

$$\delta_E \approx 0.86 \frac{r_e^3 N_e^2 \gamma}{\sigma_z(\sigma_x^* + \sigma_y^*)^2} \tag{3.1.5}$$

r_e classical electron radius
γ relativistic factor E_{beam}/m_0c^2

Beamstrahlung causes a reduction and a spread of the collision energy and can lead to undesirable experimental background. The energy loss δ_E therefore has to be limited to typically a few percent. By choosing a large aspect ratio $R = \sigma_x^*/\sigma_y^* >> 1$, δ_E becomes independent of the vertical beam size and the luminosity can be increased by making σ_y^* as small as possible. Since $\sigma_y^* = (\epsilon_{y,N}\beta_y^*/\gamma)^{1/2}$, this is achieved by both a small vertical beta function at the IP and a small normalized vertical emittance. The lower limit on β_y^* is given by the bunch length ("hourglass effect"). Setting $\beta_y^* = \sigma_z$, the luminosity can be expressed as:

$$L \approx 5.74 \cdot 10^{20}\mathrm{m}^{-3/2} \times \frac{P_b}{E_{cm}} \times \left(\frac{\delta_E}{\epsilon_{y,N}}\right)^{1/2} \times H_D \tag{3.1.6}$$

Due to the small wakefields, the superconducting linac is ideal for transporting a beam with an extremely small emittance $\epsilon_{y,N}$. In order to define a standard parameter set for the 500 GeV collider, we do not have to make full use of this potential, though. The high AC-to-beam power conversion efficiency of TESLA of about 16 % allows to produce a high beam power and to obtain the required luminosity with a total AC-power consumption of 99 MW and a normalized emittance achievable with tolerances (between 0.1 and 0.5 mm) in the linac and in the damping rings which can realistically be obtained at the time of machine installation. The additional use of beam-based correction and alignment methods will then allow to push $\epsilon_{y,N}$ to much smaller values, opening up options for upgrading the machine as schematically shown in Fig. 3.1.6. The other basic parameters, not directly entering into eq. 3.1.6, have been chosen such that freedom in parameter space is maintained, not being at a technical limit in any of the collider subsystems. For instance, the large bunch spacing (708 ns) leaves a considerable safety margin for technical components like the damping ring injection and extraction devices, bunch-to-bunch orbit measurement and correction, and for resolving single bunch crossings in the experiment. As another example, the relatively large horizontal emittance ($\epsilon_{x,N} = 1.4 \cdot 10^{-5}$m) relaxes the beam optics requirements in the damping rings. An overview of the TESLA standard parameters is given in Table 3.1.2.

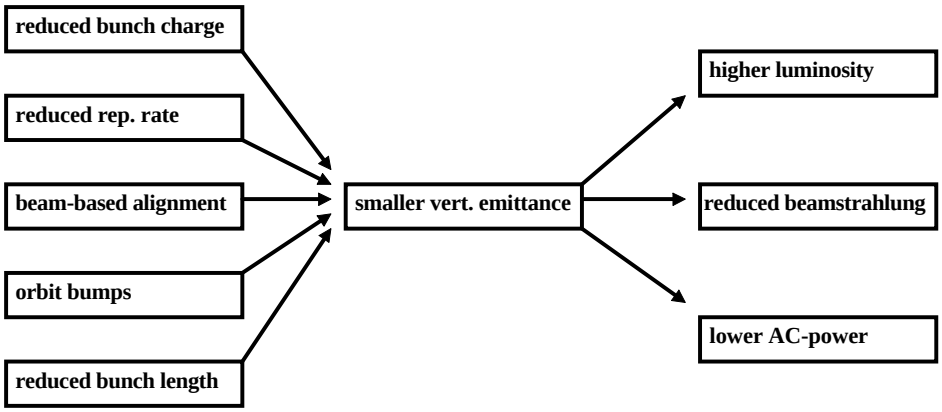

Figure 3.1.6: *Methods to reduce the vertical emittance in TESLA, and potential benefits.*

In Table 3.1.2 we also show a possible low-ϵ_y parameter set, in order to give an example for the large flexibility in parameter space available for TESLA. The version shown here combines a very low level of beamstrahlung with a somewhat higher luminosity and reduced AC-power. Such a parameter set with low δ_E would e.g. be desirable for operation around the top quark threshold (at $E_{cm} \approx 350\,\mathrm{GeV}$) or for a polarized positron source. Obtaining the small emittance will require to apply beam-based techniques, especially to improve the accuracy of the beam position monitor alignment w.r.t. the focussing magnets. The necessary accuracy (several 10's of μm, both in the linac and the damping rings) is easy to achieve and, once established, expected to be stable over long periods of time.

3.1.4 Upgrade to Higher Energy

The center-of-mass energy reach of TESLA is clearly limited by the maximum gradient achievable with the superconducting cavities and cannot, unlike designs using conventional accelerating structures, be increased by upgrading the RF-pulse power. In order to go to energies beyond $E_{cm} \approx 1\,\mathrm{TeV}$, the length of the machine would therefore have to be increased. We do believe, though, that a significant energy upgrade of TESLA will be possible within the site length for the 500 GeV design by operating the cavities at a gradient above 25 MV/m. The main reasons which justify this optimism are:

- The fundamental limit for the gradient in a Nb-structure at 2 K is well above 50 MV/m.
- Cavity tests at the TTF have shown that field emission can be very effectively suppressed and a quality factor far in excess of the design value ($Q_0 = 5 \cdot 10^9$) at 25 MV/m is feasible.
- Accelerating gradients of 30...40 MV/m [13, 14, 15] have been achieved with single-cell L-band cavities.

	Standard	Reduced ϵ_y
Accelerating gradient g [MV/m]	25	25
RF-frequency f_{RF} [GHz]	1.3	1.3
Fill factor	0.67	0.67
Total site length L_{tot} [km]	33	33
Active length [km]	20.4	20.4
# of acc. structures	19712	19712
# of klystrons	616	616
Klystron peak power [MW]	8	8
Repetition rate f_{rep} [Hz]	5	4
Beam pulse length T_P [μs]	800	800
RF-pulse length T_{RF} [μs]	1330	1330
# of bunches p. pulse n_b	1130	2260
Bunch spacing Δt_b [ns]	708	354
Charge p. bunch N_e [10^{10}]	3.63	1.82
Emittance at IP $\gamma\epsilon_{x,y}$ [10^{-6}m]	14, 0.25	12, 0.03
Beta at IP $\beta^*_{x,y}$ [mm]	25, 0.7	25, 0.5
Beam size at IP $\sigma^*_{x,y}$ [nm]	845, 19	783, 5.5
Bunch length at IP σ_z [mm]	0.7	0.5
Beamstrahlung δ_E [%]	2.5	1.0
Luminosity L [10^{33}cm^{-2}s^{-1}]	6	8.4
Beam power P_b [MW]	16.3	13
AC power P_{AC} [MW]	99	83

Table 3.1.2: *TESLA parameters for E_{cm}=500 GeV. The machine length includes a 2% overhead for energy management. The klystron power and AC power quoted include a 10% regulation reserve. The standard parameter set is the basis for the design study documented in this report. The additional parameter set (right-hand column) is given as an example for the potential of TESLA operating with a lower beam emittance.*

We are aware that a number of questions have to be adressed before a definite conclusion can be drawn (e.g. stronger Lorentz-force detuning, potentially more severe dark current problems), but with further R&D it seems conceivable that a maximum gradient of about 40 MV/m at $Q_0 = 5 \cdot 10^9$ can be reached with the 9-cell cavities. The average gradient for the entire linac may be lower initially, so that a possible scenario for an energy upgrade in steps could be to exchange groups of modules containing the "weakest" (i.e. lowest gradient) cavities with new, high-performance modules. This upgrade path leads to a maximum energy of E_{cm}=800 GeV. The subsystems for TESLA (in particular the beam delivery system) are designed such that the energy upgrade can be accomodated without further hardware modifications. In order to obtain optimum luminosity at higher energy, an upgrade of the RF-system is also necessary, though. At higher gradient, either the RF-pulse power or pulse length must be increased to maintain a reasonable ratio of beam-on time to RF-on time. We follow the first ap-

	800 GeV	800 GeV low ϵ_y	1.6 TeV
Accelerating gradient g [MV/m]	40	40	40
Total site length L_{tot} [km]	33	33	≈ 62
Active length [km]	20.4	20.4	40.8
# of acc. structures	19712	19712	39424
# of klystrons	1232	1232	2464
Klystron peak power [MW]	8	8	8
Repetition rate f_{rep} [Hz]	3	3	3
Beam pulse length T_P [μs]	640	640	640
RF-pulse length T_P [μs]	1330	1330	1330
# of bunches p. pulse n_b	1130	2260	2260
Bunch spacing Δt_b [ns]	566	283	283
Charge p. bunch N_e [10^{10}]	3.63	1.82	1.82
Emittance at IP $\gamma\epsilon_{x,y}$ [10^{-6}m]	14, 0.25	12, 0.025	12, 0.025
Beta at IP $\beta^*_{x,y}$ [mm]	25, 0.7	25, 0.5	25, 0.5
Beam size at IP $\sigma^*_{x,y}$ [nm]	669, 15	618, 4.0	436, 2.8
Bunch length at IP σ_z [mm]	0.7	0.5	0.5
Beamstrahlung δ_E [%]	5.2	2.2	6.7
Luminosity L [10^{33}cm^{-2}s^{-1}]	5.7	11	20
Beam power P_b [MW]	15.6	15.6	31.2
AC power P_{AC} [MW]	115	115	230

Table 3.1.3: *TESLA parameters for an upgrade to 800 GeV and for a 2nd stage at 1.6 TeV with doubled linac length (see text).*

proach, which has the advantage that the modulators providing the pulse power for the klystrons do not have to be modified. The 800 GeV version of TESLA would then have twice as many klystrons and modulators as the initial stage at 500 GeV. The pulse repetition rate is reduced so that the dynamic load for the cryogenic system remains almost constant and the AC-power consumption is only slightly increased. As in the previous section, we show two sets of beam parameters in Table 3.1.3. The alignment tolerances in the damping rings and in the main linac are for both versions similar as for the respective parameter sets of TESLA-500.

The potential for operating with a very small vertical beam emittance becomes particulary important when we consider a linear collider at energies beyond 1 TeV. According to eq. 3.1.6, scaling the luminosity as $L \propto E^2_{cm}$, as desirable, becomes difficult unless a high level of beamstrahlung is accepted. Assuming that the same vertical emittance as for the 800 GeV low-ϵ_y version can be maintained in a machine doubled in length, we arrive at the parameter set for a 1.6 TeV collider shown in the last column of Table 3.1.3. It demonstrates that the TESLA approach has the capability of maintaining reasonable interaction parameters at an energy scale well above 1 TeV. We have not yet investigated this 2nd stage upgrade in detail, but several aspects are already included in the initial stage design. The tunnel is kept straight in the beam

delivery section, so that it can later be used for the installation of linac structures. The two linacs of the 1st stage would be used as one linac of the 2nd stage (note that the superconducting cavities allow to accelerate a beam in both directions) and the machine length be extended to one side. Thus the part of the linac being used for the FEL facility and potentially other options would remain unchanged. A new beam delivery system and interaction region would have to be constructed. The entire injection system can be kept basically unchanged, except for modifications concerning the spent beam capture system and an additional transfer line from one of the damping rings to the beginning of the new 800 GeV linac.

Bibliography

[1] G. A. Loew (ed.), *International Linear Collider Technical Review Committee Report*, SLAC-R-95-471, 1995.

[2] D. Burke for the FFTB Collaboration, *Results from the Final Focus Test Beam*, Proc. of the IVth European Particle Accelerator Conf., London 1994, Vol. I, p. 23.

[3] R. Brinkmann, *Beam Dynamics in Linear Colliders- What Are the Choices ?*, DESY-M-95-10, 1995.

[4] *Proposal for a TESLA Test Facility*, DESY-TESLA-93-01, 1992.

[5] C. Crawford et al., Particle Accelerators 49, p. 1, 1995.

[6] D. A. Edwards (ed.), *TESLA Test Facility Linac - Design Report*, DESY-TESLA-95-01, 1995.

[7] J.M. De Conto (ed.), *Electron Laboratory for Europe - Accelerator Technical Proposal*, 1993.

[8] M. Tigner, B. H. Wiik and F. Willeke, Proc. Particle Accelerator Conf., San Francisco 1991, Vol. 5, p. 2910.

[9] Z. Z. Aydin et al., *HERA+LC Based γp Collider: Luminosity and Physics*, DESY-95-014, 1995.

[10] R. Brinkmann and M. Dohlus, *A Method to Overcome the Bunch Length Limitation on β_p^* for Electron-Proton Colliders*, DESY-M-95-11, 1995.

[11] *$\mu^+\mu^-$ Collider – A Feasibility Study*, BNL-52503, FNAL-Conf.-96/092 and LBNL-38946, July 1996.

[12] P. Chen and K. Yokoya, *Beam-Beam Phenomena in Linear Colliders*, KEK-report 91-2, 1991.

[13] T. Higuchi et al, *Investigation of Barrel Polishing for Superconducting Niobium Cavities*, KEK-report 95-220, 1996.

[14] P. Kneisel, R. W. Röth and H.-G. Kürschner, *Results from a Nearly "Defect-Free" Niobium Cavity*, Proc. 7th Workshop on RF-Superconductivity, p. 449,Saclay 1995.

[15] M. Ono, S. Noguchi, K. Saito, E. Kako, T. Shishido, H. Inoue, Y. Funahashi, T. Fujino, S. Koizumi, T. Higuchi, T. Suzuki, H. Umezawa and K. Takeuchi, *Achievement of High Acceleration Field (40 MV/m) in L-Band Superconducting Cavity at KEK*, Proc. 21st Linear Accelerator Meeting, Tokyo 1996, NUP-A-96-10, p. 38.